NACA RM L50F27a

NACA

RESEARCH MEMORANDUM

INVESTIGATION OF AN IMPULSE AXIAL-FLOW COMPRESSOR ROTOR OVER A RANGE OF BLADE ANGLES

By Wallace M. Schulze, John R. Erwin, and Willard R. Westphal

Langley Aeronautical Laboratory
Langley Air Force Base, Va.

NATIONAL ADVISORY COMMITTEE
FOR AERONAUTICS

WASHINGTON

August 29, 1950

NATIONAL ADVISORY COMMITTEE FOR AERONAUTICS

RESEARCH MEMORANDUM

INVESTIGATION OF AN IMPULSE AXIAL-FLOW COMPRESSOR ROTOR OVER A RANGE OF BLADE ANGLES

By Wallace M. Schulze, John R. Erwin, and Willard R. Westphal

SUMMARY

An investigation was made to study the performance characteristics of an impulse axial-flow compressor rotor over a wide range of operating conditions. The high-turning-angle low-static-pressure-rise rotor reported in NACA RM L9J05a was tested with constant annulus area at several values of blade-angle settings in addition to the one for which it was designed. A large range of quantity rates of flow was used in testing, and special attention was given to stall conditions.

A maximum total-pressure-rise coefficient of 3.00 at 93 percent efficiency was obtained with a static-pressure-rise coefficient of -0.49 by operating at a blade-angle setting 18° above the design value. A maximum static-pressure coefficient of 0.53 at 90 percent efficiency was obtained with a total-pressure coefficient of 1.64 using a blade angle 9° below design. At the blade-angle setting and quantity-flow coefficient of the original design, a total-pressure coefficient of 2.10 and a static-pressure coefficient of 0.39 were obtained with an efficiency of 93 percent. This investigation also produced new information on the stall characteristics of impulse blading and on the conditions under which the rotor would induce steady flow.

INTRODUCTION

The investigation of reference 1 was made to determine the possibilities of obtaining high total-pressure coefficients by applying a constant-pressure, high-turning principle to the design of an impulse axial-flow compressor rotor. The rotor was designed to operate with an inlet air angle relative to the rotor β_1 of 45° and a turning angle θ of 75°. The static pressure across the rotor was maintained constant by a 20-percent decrease in annular area through the blades, so that at these low test speeds, the axial velocity increased about 20 percent through the rotor. A total-pressure coefficient of 2.3 was obtained

with a rotor efficiency of 98.3 percent. This rotor was also tested with stator blades installed downstream. In this investigation, the performance of the test compressor was measured over a range of quantity-flow coefficients at a constant speed of 1200 rpm with the rotor blades set at the design angle.

The design of an efficient axial-flow compressor stage in which a considerable increase in axial velocity across the rotor occurs is difficult because the velocity entering the stators is high and the entire static-pressure rise must be produced by the stator. Such stages do not lend themselves readily to multistaging since the relative velocities reach prohibitive values in a few stages. The present investigation was intended to determine whether high turning angles and high total-pressure coefficients could be obtained when the rotor produces a significant static-pressure rise. The rotor used was the same as that tested in the investigation reported in reference 1, except that the annulus area through this rotor was maintained constant. In these low-speed tests, therefore, a virtually constant axial velocity and an increasing static pressure were obtained. In addition, further information was desired as to the ability of impulse rotors to induce a flow in the desired direction.

To obtain this information, the impulse rotor was tested over a wide range of blade-angle settings, from 9° below to 24° above the original design setting. Performance measurements were made for each of these conditions at a constant quantity-flow coefficient. At three blade-angle settings, corresponding to the design condition and to the upper and lower limits of useful operating range, the performance of this rotor was determined over a range of quantity-flow coefficients. The stalling phenomena were investigated in some detail for 11 blade-angle settings.

SYMBOLS

D	diameter, feet
h	blade height, feet
m	mass rate of flow, slugs per second
n	rotor speed, revolutions per second
p_t	total pressure, pounds per square foot
p_s	static pressure, pounds per square foot
Q	quantity rate of flow, cubic feet per second

q	dynamic pressure, pounds per square foot
r	radius, feet
U	velocity of rotor blades, feet per second
V	velocity of air (relative to casing), feet per second
W	velocity of air (relative to rotor), feet per second
α	angle of attack, degrees
α_d	design angle of attack, 43° at inboard section, 25 percent of blade height from hub
β	stagger angle, degrees (see fig. 1)
η	adiabatic efficiency
θ	turning angle, degrees
ρ	air density, slugs per cubic foot
ζ	blade-angle setting, degrees
ζ_d	design blade-angle setting, (see fig. 1)
Φ	quantity-flow coefficient $\left(\frac{Q}{nD_t^3}\right)$
Φ_d	quantity-flow coefficient at which α_d is obtained
φ	angle of air flow with reference to the rotor axis in stationary coordinates, degrees
ψ_s	static-pressure-rise coefficient $\left(\frac{\Delta p_s}{\frac{1}{2}\rho U_t^2}\right)$
ψ_t	total-pressure-rise coefficient $\left(\frac{\Delta p_t}{\frac{1}{2}\rho U_t^2}\right)$

Subscripts:

a	axial direction
i	inboard section
o	outboard section
t	tip
tan	tangential
1	station upstream of rotor blades (see fig. 2)
2	station downstream of rotor blades (see fig. 2)

APPARATUS AND TESTS

The 75-horsepower low-speed test compressor used in the previous investigation as modified for these tests is indicated in figure 2. The initial rotor tip clearance was approximately 0.012 inch, or less than one-half percent of the blade height. A test run was made with the original blade setting at design quantity flow $\Phi_d = 0.80$. Without disassembling the rotor, the 3-inch-long blades were trimmed to give a tip clearance constant from leading edge to trailing edge at ζ_d of approximately 0.090 inch (3 percent h), and the same test was repeated. This large clearance was needed for later tests to keep the blade-tip corners from striking the outer casing at high blade angles. Comparison of these two runs indicated the effect of greater clearance. Flow surveys were made at stations 1 and 2, one-half chord fore and aft of the rotor, using instruments of type I (reference 1). Performance tests, as described in reference 1, were run at 1000 rpm. Those investigating starting and stalling phenomena were run at various speeds.

Flow-inducing tests.- A number of tests were made to determine the range of blade-angle settings ζ for which the rotor would induce flow in the desired direction. In addition, information concerning the usable operating range of ζ was obtained. The starting, running, and stalling characteristics of the rotor were observed at 3° increments of ζ, from 9° below the design value, $\zeta_d - 9^\circ$, to 24° above design, $\zeta_d + 24^\circ$. The performance of the rotor was measured at an approximately constant quantity-flow coefficient, $\Phi \cong 0.80$ for all of these ζ values, except $\zeta_d + 24^\circ$ for which steady flow could not be obtained.

Performance tests over a range of flow coefficients for three blade settings.- Performance tests were made over a range of quantity-flow coefficients Φ for the design blade setting angle ζ_d and for the upper and lower limits of the practical operating range, $\zeta_d + 18^\circ$ and $\zeta_d - 9^\circ$, respectively (fig. 3). At ζ_d, seven runs were made covering the range of Φ from near stall to well above the design condition ($\Phi = 0.54$ to 1.01). The tests at $\zeta_d + 18^\circ$ were similar, but at this condition the maximum Φ obtainable with the existing test equipment was 0.90 which was considerably below the 1.56 value needed to give the design angle of attack. The design angle of attack was defined as 43° at the inboard section for all values of ζ.

At $\zeta_d - 9^\circ$, tests were made with relatively large values of Φ up to 1.12 in addition to the usual range. This was done so that operation under conditions of negative stall, a flow separation that occurs on the concave surface of the blade at very low angles of attack, might be observed.

Stall tests.- For the stall investigation, flow directions relative to the rotor were indicated by small nylon tufts glued to the rotor and blade surfaces and to threads stretched between blades. Approximately 60 tufts were used. Three threads with five tufts on each were stretched between adjacent leading edges at three radial positions. Three similar threads were stretched between adjacent trailing edges. Two threads were suspended between blades at about the 50-percent-chord point at one-third and two-thirds of the blade height from the blade root section. Ten or twelve tufts were glued to both convex and concave blade surfaces. The tufts were spread over many blades so that no tuft was in the wake of another tuft or thread. Flow directions in stationary coordinates were indicated by tufts glued to the inner case upstream and downstream of the rotor. The tufts were illuminated with intense stroboscopic lights placed far upstream and far downstream of the rotor and triggered by a contactor on the rotor shaft. The tufts were observed through transparent ports in the test blower outer case.

As is discussed hereinafter, under certain conditions the flow fluctuations had periodic characteristics and for such cases the frequency was measured by illuminating the tufts on the inner case with a Strobotac. The quantity-flow coefficient Φ was determined by comparison of q_1 values taken upstream of the rotor at the mean diameter with a curve of q_1 versus Φ obtained from complete surveys. The Φ values computed by this method may be in error as much as 10 percent or more during surging operation, but are considered to be sufficiently accurate to provide a qualitative picture of stall phenomena.

RESULTS AND DISCUSSION

All performance values presented were calculated from flow survey data by the methods described in reference 1. As in that investigation, the static-pressure readings of the instruments were calibrated to an accuracy of ±0.2 percent of the dynamic pressure, and the direction readings were accurate to $\pm 1/4^{\circ}$. The efficiency was corrected for differences in the mass flows measured at stations 1 and 2, as described in reference 1. The results presented are believed to be reliable to within 1 or 2 percent. Figures 4 and 5 present the differences in mass flow measured at the two stations to show their magnitude and give an indication of the accuracy of this work.

General Operating Characteristics

Starting and running.- In reference 1, the assumption was made that the rotor could not induce a flow in the desired direction unless the entrance air direction β_1 had a larger inclination from the axis than the exit air direction β_2. A second assumption was that the leading edge of the rotor blades should precede the trailing edge in the direction of rotation. This second assumption is based upon the supposition that the flow will pass through the blades from the side at which the blade mean line makes the larger angle from the axis. Therefore, with circular-arc mean-line blades, as used in this investigation, the direction of flow would depend upon which edge preceded in the path of rotation. An advancement of the blade angle more than 2° above ζ_d would cause the trailing edge to precede at the inboard section (located 25 percent h from the hub) or an angle increase more than $11\frac{1}{2}^{\circ}$ would do the same for the outboard section (25 percent h from the tip). If this second assumption is valid, the angle above which flow would not be induced in the desired direction would be within this approximate range.

The rotor was tested with a large range of blade-angle settings, $\zeta_d - 9^{\circ}$ to $\zeta_d + 24^{\circ}$, to determine the starting and running behavior. At the lowest blade angle tested, $\zeta_d - 9^{\circ}$, the total- and static-pressure-rise conditions through the test section were similar to conditions in the usual axial-flow compressor. The starting and running characteristics were also found to be similar.

Hysteresis in starting was observed; that is, larger throttle settings were necessary to start with unstalled flow than the settings that were used to reduce the flow to the stall point after smooth flow had been established. The flow started simultaneously with the rotor

and continued smoothly over a wide range of Φ. At blade-angle settings several degrees higher, the test compressor showed very little change in general behavior.

At $\zeta_d + 12^\circ$, some changes in the starting characteristics occurred. At this blade angle and all higher ones to $\zeta_d + 21^\circ$, no hysteresis of the flow was observed, and the test compressor would start with steady flow if the throttle position was set at or above the minimum point for unstalled operation, approximately $1/2\ \Phi_d$ or above. Thus, when starting the throttle did not have to be opened beyond the minimum point as is necessary in the case of conventional axial-flow compressors. However, the starting of the air flow was observed to lag behind that of the rotor and at the next blade setting, $\zeta_d + 15^\circ$, this tendency was more pronounced. Under usual operating procedure, in which the rotor was brought up to speed in 10 to 15 seconds, the flow began several seconds after the rotor began rotating and did not reach a steady state until several seconds after the rotor reached test speed. This delayed-starting tendency was even more evident at 18° above ζ_d, taking approximately 10 seconds at 1000 rpm, or 20 seconds at 500 rpm to start flowing. Once started, the flow increased rapidly to a steady-state condition. After the flow reached steady-state conditions, the operation of the compressor was quite normal, a change of flow rate occurring simultaneously with a change in rotor speed. The 18° above ζ_d condition was the lowest setting tested at which all points of the trailing edge preceded any point of the leading edge in the direction of rotation.

At 21° above ζ_d (fig. 6), when the rotor speed was brought up to 500 rpm, there appeared to be no axial air flow present. However, smoke introduced at the exit indicated a slow drift of air in the reverse direction. When the rotor speed was increased to 1000 rpm, the reverse flow became unsteady and started surging. At each surge, some air was observed going in the desired direction for a short time. After one of these surges, a small flow in the desired direction persisted, and then rapidly increased to the usual rate. After the flow was established, it remained smooth and stable throughout a range of quantity flows and rotor speeds.

At $\zeta_d + 24^\circ$, a steady flow in the desired direction could not be established. During operation at 1000 rpm, the air flowed slowly in the reverse direction with an occasional surge that caused a momentary flow in the desired direction. Doubling the rotor speed increased the violence of the surges, but the flow would not continue in the desired direction. It is believed that, if flow had been established by external means, the flow probably would have continued, but facilities were not available to try this.

It was desired to determine the validity of the first design assumption of reference 1, that, to induce the flow in the desired direction, the entering stagger angle should be greater than the exit stagger angle. To do this, a determination was made of the entrance and exit air direction relative to the rotor at the mean diameter of the annulus for all tests. It was found that the entrance air direction had a larger inclination from the rotor axis than the exit air direction ($\beta_1 > \beta_2$) for all tests except the one with a blade-angle setting at 21° above design. Even then, nearly half the blade was operating with $\beta_1 > \beta_2$. It is apparent that the main design assumption concerning flow-inducing criteria was satisfied.

Applying the second design assumption of reference 1 concerning the effect of the relative position of the leading and trailing edges on the flow-inducing ability of the rotor, blade-angle settings above $11\frac{1}{2}^\circ$ would not be expected to induce flow in the desired direction. However, the rotor was able to induce such flows at blade settings well above this value; consequently, it appears that the airfoil shape and the inlet- and outlet-passage configuration had a favorable effect on the ability of the rotor to induce the desired flow.

Pressure-rise stalling at low blade angles.- At low blade-angle settings, $\zeta_d - 9^\circ$ to $\zeta_d + 3^\circ$, there was a static-pressure rise across the rotor at all diameters as in the conventional axial-flow compressor and the stall phenomena were similar to those previously observed in a conventional compressor in an unreported investigation. In both cases, the unsteady flow that occurred during stalled operation was due to reversed flow through a region occupying approximately 15 to 40 percent of the annulus circumference and area, and extending from the entrance cone through the rotor and into the diffuser. This region of reversed flow rotated about the annulus with the angular velocity of the air downstream of the rotor and the rotor blades passed through the region of reversed flow. In the impulse blower, the region rotated faster than the rotor blades. In the conventional compressor, the opposite was true. This flow pattern was observed in the impulse compressor at the Φ and ζ values indicated in figure 7. The quantity coefficient at which smooth flow changes to surging flow varies from about 75 percent Φ_d at $\zeta_d - 9^\circ$ to 40 percent Φ_d at $\zeta_d + 15^\circ$.

The reversed flow is believed to be started and maintained in the following manner: As the compressor is throttled to the stall point, the flow separates from the convex surface of one blade or a group of blades because of the large adverse pressure gradient on this surface. Ideally, this separation should occur on all blades simultaneously, but a slight difference in blade shape, blade-angle setting, or entrance

air direction causes one or a group of blades to separate first. Separation reduces the effective passage area at the exit of the stalled passages, increasing the velocity and thereby decreasing the static pressure behind the stalled blades to a value below that existing behind the adjacent unstalled blades. The higher-pressure air behind the unstalled passages is accelerated towards the low-pressure region and moves upstream into the separated layer of air which almost instantly thickens the layer until it constricts the entire blade-passage exit. Simultaneously, the air stream entering the blade passage is diverted, and reverse flow occurs through the entire blade passage and extends forward into the entrance cone. The reversed flow increases the axial velocity required throughout the remainder of the annulus for the same net flow out the throttle, and so reduces the angle of attack and static-pressure rise. A stable condition of flow exists. As the throttle is closed further, a larger portion of the annulus is occupied by the reversed flow. This permits the axial velocity over the unstalled blades and, therefore, also the angle of attack to remain more or less constant even though the flow passing through the throttle is diminished.

Pressure-drop stalling at high angles.- The flow pattern described above cannot occur unless there is a static-pressure rise across the rotor. Unlike the conventional compressor, the impulse compressor has a static-pressure drop across the rotor at root and mean diameter sections when operating at high blade-angle settings. Figure 8 shows the pressure-rise coefficients measured at the mean diameter at the smallest quantity flow that could be obtained without stalling. The stall phenomena were found to be quite different at the high blade-angle settings from those observed at the low blade-angle settings. At blade angles of more than $\zeta_d + 18^\circ$, the flow was free of pulsations or surging over a much wider Φ range than at lower angles. As the flow was reduced to small quantities by throttling, the separation point moved forward on the convex surface until the flow over the entire blade surface was separated. The total-pressure rise decreased rapidly, but there was no surging even though the angle of attack at the inboard section increased about 60° above α_d. At a blade-angle setting 21° above design, the flow was separated from the convex surface at the highest quantity flow that could be obtained with the existing test apparatus, $\Phi = 0.77$. Surging with reverse flow did not begin until Φ was reduced to 3 percent of Φ_d (fig. 7). Although the static pressure decreased through the rotor at root and mean diameter, reversed flow was possible because of the static-pressure rise at the tip section due to centrifugal force.

Stalling at intermediate blade angles.- At the intermediate blade angles, from $\zeta_d + 6^\circ$ to $\zeta_d + 18^\circ$, regions of both pressure-rise and pressure-drop stall were observed as indicated in figure 7. Reducing the quantity-flow rate by throttling to Φ of about 0.6 resulted in a static-pressure-rise stall with surging similar to that observed at the

low values of ζ. This surging decreased in severity, however, when Φ was further reduced to about 1/4 Φ_d; at this point surging stopped and steady flow, pressure-drop stalling, similar to that described for high values of ζ, was established. The pressure-drop stalling continued until the quantity-flow rate was reduced to very small values, 3 to 8 percent Φ_d, depending upon ζ (fig. 7). Then surging stall began again and continued to $\Phi = 0$. Pressure-drop stalling was first observed over a small range of Φ at $\zeta_d + 6^\circ$, and occurred over an increasing range of Φ as ζ increased.

Further remarks.- The information obtained in the present investigation suggests that a possible flow pattern of pressure-rise stall in conventional (reaction) compressors is not a separated region retaining its position with relation to a particular blade, but is a reverse flow which rotates with the tangential velocity downstream of the rotor. This flow pattern was clearly evident in the impulse compressor (this investigation used only a rotor) when operating with a static-pressure rise, and in a conventional compressor rotor having a guide vane row upstream. In both cases, when reverse flow first occurred through the test section, the flow discharging from the throttle was only slightly unsteady, indicating that, initially, this was a stable flow condition. The flow remained stable as the rate of flow was reduced until a large percentage of the annulus contained reversed flow. Separation in all blade passages probably did not occur until the mean static-pressure rise across the rotor became so small that the reverse flow could no longer be sustained. If a compressor can be designed to permit reversed flow without prohibitive turbulent mixing losses, a significant gain in operating range at full speed might be achieved. An obvious possibility is to recirculate some of the flow externally.

The smooth operation of the impulse rotor in the pressure-drop-stall regime provides information as to the probable behavior of the rear stages of a conventional compressor at low rotational speed or at high mass flow at design speed. In these cases, the rear blading receives the flow at negative angles of attack and a drop in pressure occurs. At high negative angles, blade stall similar to that observed in the impulse compressor occurs, but the flow continues to pass through the blades without surging. If means to permit recirculation of some of the flow were provided, a higher pressure ratio could be obtained at low speeds, as the angle of attack of the blades in the rear stages would be increased and that of the forward stages decreased. A gain in the torque available for the acceleration of turbojet or turbo-propeller engines might be realized by this external recirculation system for increased operating range at full speed.

Rotor Performance at Constant Quantity Coefficient

Effect of blade-tip clearance.- Two tests were made at the design blade-angle setting as an indication of the effect of blade-tip clearance on rotor performance. At the low tip clearance of approximately 1/2 percent blade height, an efficiency of 95.3 percent, a total-pressure-rise coefficient of 2.10, and a static-pressure-rise coefficient of 0.49 were obtained (figs. 9 and 10). The results of the test with a blade-tip clearance of 3 percent h showed no change in the total-pressure-rise coefficient, but the measured efficiency was 93.1 percent and the static-pressure-rise coefficient was 0.39. Although these results indicate a higher efficiency with low blade-tip clearances, the difference in the two measured values has about the same order of magnitude as the scatter present in the results of efficiency plotted against blade-angle setting in figure 9, and so are not conclusive. The decrease in static-pressure-rise coefficient with increased clearance appears more definite as shown by figure 10.

Reference 2 reports an investigation of tip-clearance effects for an axial-flow system having a rotor and stator. The results of that work indicate a drop in efficiency with increased tip clearance having the same order of magnitude as is presented in the preceding paragraph. Reference 2 also indicated a decrease in total-pressure rise with increased tip clearance, but in the present investigation the expected change was not measured, probably due to inaccuracies of measurements or calculations.

Effect of blade angle.- A constant quantity-flow coefficient Φ of 0.80 was intended for all flow-inducing tests, but because of practical difficulties the actual test values varied from 0.77 to 0.84. This variation was not believed serious. The efficiencies measured for the various values of ζ are presented in figure 9. The faired curve indicates that the peak efficiency was 94 percent at $\zeta_d + 4^\circ$, diminishing slowly with increasing ζ and more rapidly with decreasing ζ. Although the blades were operating at off-design conditions both above and below ζ_d, a high efficiency resulted at all the positive angles tested except $\zeta_d + 21^\circ$, because ψ_s diminishes and becomes negative with increasing ζ (fig. 10). The flow at $\zeta_d + 21^\circ$ was partially separated and therefore contained additional losses.

A constant Φ, as used in this group of tests, causes a higher angle of attack α and consequently a higher turning angle θ with each increase in ζ. Figure 11 presents α and θ values plotted against ζ measured at the inboard and outboard design blade sections. The higher θ results in a rising total-pressure coefficient ψ_t with increasing blade angle (fig. 10). The static-pressure coefficient ψ_s however, shows the opposite effect, decreasing with increasing ζ. This

result is due to the increased exit stagger angle and decreased exit flow area (higher exit velocity). Although a high ψ_t is desirable, an associated ψ_s drop increases the difficulty of the stator problem. Thus, a high positive ratio of ψ_s to ψ_t is generally desirable for most applications using both rotors and stators.

Rotor Performance with Varying Quantity-Flow Coefficient

The performance of the impulse rotor at various values of quantity-flow coefficient Φ was measured for the design, 18° above design and 9° below design blade-angle settings. These tests were made at the upper and lower limits of useful operating ζ range and the design blade-angle setting, permitting comparison with reference 1. Figure 12 shows the range in angles of attack α and turning angles θ covered in these tests. In the tests, at $\zeta_d - 9^\circ$ a minimum α of 19.3° with a corresponding θ of 49.1° was measured at the outboard section. The results of the tests at $\zeta_d + 18^\circ$ gave a maximum α of 75.2° with a θ of 117.0° at the inboard section. These results, for a single blade design, indicate that impulse compressors having proper blade camber can be designed to operate satisfactorily with turning angles from 50° to 120°.

High blade-angle setting.- The tests at $\zeta_d + 18^\circ$ show a significant increase in total-pressure-rise coefficients ψ_t over those presented in reference 1. At a quantity-flow coefficient Φ of 0.90, a ψ_t of 3.0 (fig. 13) with an efficiency η of 93.2 percent (fig. 14) was measured. This Φ was far below the value needed to establish the design angle of attack of the blades $\Phi_d = 1.56$ (fig. 7), but was the largest that could be obtained. The rapid drop in η below Φ of 0.8 is attributed to flow separation from the blades at that very high angle of attack, about 17° above α_d. The favorable static-pressure gradient (fig. 13) probably reduced the extent of the separation.

Design setting.- The tests made at ζ_d are compared in figures 13 to 15 with those in reference 1 to show the effect of removing the area change in the blade passages and increasing the tip clearance. The average turning angles and the velocity of the air leaving the rotor were decreased by increasing the passage exit area, and consequently the total-pressure rise was reduced (fig. 13). The larger exit area resulted in more diffusion in the passages and increased the static-pressure-rise coefficient from 0.20 to 0.38 at the design quantity-flow rate of 0.80. The efficiency curve was flat as before, but the flow losses from increased rate of diffusion and the larger blade-tip clearance lowered the design point efficiency from 98.3 to 92.7 percent (fig. 14).

Low blade-angle setting.- The test results at $\zeta_d - 9^\circ$ were similar to those of more conventional axial-flow rotors, even though the turning angles measured, 50° to 80° (fig. 12), were comparatively high. If the optimum angle of attack for this setting is assumed to be the same as that for ζ_d, $\alpha_d = 43^\circ$ at the inboard station, the Φ_d would be 0.58. At this flow rate, the measured static-pressure-rise coefficient ψ_s was 0.53, an increase of about 40 percent over the value measured at peak efficiency for ζ_d. The maximum ratio of ψ_s/ψ_t measured, 0.32, identifies this rotor configuration as a reaction type. In figure 16, the ψ_s/ψ_t ratios measured at $\zeta_d - 9^\circ$ are compared with values obtained for ζ_d and $\zeta_d + 18^\circ$ settings. Although the ψ_s/ψ_t ratios are largest for the low-angle tests, the values of ψ_s for 9° below ζ_d are nearly the same as those at ζ_d (fig. 13). The explanation was evident after a study of the flow geometry.

In all tests, including various values of ζ and Φ, the air left the blade passages at a stagger angle approximately 10° lower than the mean-line angle of the blade trailing edge. Consequently, reducing the blade angle to $\zeta_d - 9^\circ$ decreased the exit stagger angle from 30° to 21° at the inboard section and from 17.5° to 8.5° at the outboard section. In this constant-annulus-area, low-speed rotor, ψ_s depended almost wholly upon the ratio of the $(\text{cosines})^2$ of the entrance and exit stagger angles. At similar quantity-flow rates, the entrance stagger angles were the same, so that the exit stagger angles and boundary-layer thickness determined ψ_s. Since the cosines of small angles are near 1, the cosines for the low exit stagger angles given previously show little variation (at the mean diameter, $\cos 23.75^\circ = 0.915$, $\cos 14.75^\circ = 0.967$); furthermore, the effect of the boundary layer tended to nullify the area increase.

Therefore, ψ_s for the low and design ζ tests was nearly the same and the two curves on figure 13 closely correspond. By this same explanation, lower ζ tests were regarded as unnecessary because significantly larger ψ_s would probably not have been realized. Further, the stagger angle at which α_d would result at the outboard station for this setting was 57.4°, a fairly high value. Larger ψ_s/ψ_t ratios would be obtained largely by virtue of a decrease in ψ_t, as indicated by the trends of these low-angle tests. The region of negative slope in the ψ_t curve for the $\zeta_d - 9^\circ$ configuration (fig. 13) shows a characteristic of the test compressor at this low value of ζ that is common to more conventional axial-flow compressors.

The peak efficiency of the $\zeta_d - 9^\circ$ tests had a value of 90.6 percent at approximately 0.65 quantity-flow coefficient (fig. 14). At this Φ, the angle of attack of the blades was 2.7° less than α_d. The reduced efficiency at higher flow rates was probably due to a flow separation on the concave blade surface, that is, a negative stall. The effect of the consequent large wakes was a reduction of the measuring accuracy. This is illustrated in figure 5 by the large difference between m_2 and m_1 for the high Φ values.

General summation.- The ability of the impulse rotor to turn flow efficiently 75° from an entering stagger angle of 45° while operating with constant axial velocity and a static-pressure rise, indicates an increased utility for this type of compressor. The annulus of an impulse compressor does not necessarily have to contract through the rotor blades. This makes the design and construction of a multistage impulse compressor more like conventional axial-flow machines. Maintaining the axial velocity constant increases the static-pressure rise through the rotor, removing some of the burden from the stator blades. The design of an efficient stator is made less difficult because the velocity entering the stationary rows is reduced. Some penalty in reduced total-pressure coefficient is incurred by the use of constant axial velocity as is a slight reduction in rotor efficiency. The rotor efficiency loss may be offset by reduced stator losses, however.

An extrapolation of the data from the low-speed tests to high-speed operation using the same method and entrance conditions as those used in reference 1 (Mach number relative to rotor, 0.60; no guide vanes; tip speed 540 fps) indicates that the stator Mach number using constant axial velocity would be 0.718. Assuming the same stage efficiency reported in reference 1, 89.6 percent, a stage total-pressure ratio of 1.36 is predicted. The use of constant axial velocity rather than constant static pressure at the inboard station results in a 10-percent decrease in the Mach number entering the stator and also a 10-percent decrease in the stage total-pressure rise.

CONCLUSIONS

As a result of the series of tests made on the impulse axial-flow rotor having a 3-percent blade-tip clearance with various blade setting angles and quantity-flow rates, and with constant axial velocity through the rotor, the following specific conclusions were reached:

1. The design of an impulse axial-flow compressor is not nearly so exacting as originally supposed. The impulse rotor will operate throughout a wide range of conditions with behavior similar to that of a more

conventional axial-flow compressor. A wider range of application for impulse compressors appears possible than might have been concluded from NACA RM L9J05a.

2. The impulse rotor will operate efficiently with reasonable static-pressure rise. The highest static-pressure-rise coefficient ψ_s obtained was 0.53 at a quantity-flow coefficient Φ of 0.56, total-pressure-rise coefficient ψ_t of 1.64, and an efficiency η of 90 percent at the blade-angle setting 9° below the original design value, $\zeta_d - 9^\circ$.

3. The impulse rotor will efficiently produce very high total-pressure-rise coefficients. The highest total-pressure-rise coefficient of 3.00 and the maximum turning angle of 117° at the inboard section occurred at a Φ of 0.90, ψ_s of -0.49, η of 93 percent at the $\zeta_d + 18^\circ$ blade-angle setting.

4. At the blade-angle setting and quantity-flow coefficient of the original design a total-pressure coefficient of 2.10, and a static-pressure coefficient of 0.39 were obtained with an efficiency of 93 percent.

5. The impulse rotor will operate without surging at flow rates as low as 75 percent of the design quantity-flow rate Φ_d, at the 9° below design blade-angle setting $\zeta_d - 9^\circ$, and to about 40 percent of Φ_d at $\zeta_d + 15^\circ$. Between 6° and 18° above ζ_d, the surging in the stall range is very mild and the rotor is able to operate at a stable flow rate as low as 8 to 4 percent of Φ_d, depending upon the blade-angle setting.

6. The impulse rotor will induce its own flow at any condition for which, when operating, the air entering the rotor has a larger average inclination from the rotor axis than the air leaving it ($\beta_1 > \beta_2$).

7. Increasing the tip clearance of the impulse rotor blades from 0.50 percent to 3.0 percent had a negligible effect on the total-pressure-rise coefficient, little effect on the efficiency, but reduced the static-pressure-rise coefficient from 0.49 to 0.39.

Langley Aeronautical Laboratory
National Advisory Committee for Aeronautics
Langley Air Force Base, Va.

REFERENCES

1. Erwin, John R., and Schulze, Wallace M.: Investigation of an Impulse Axial-Flow Compressor. NACA RM L9J05a, 1950.

2. Ruden, P.: Investigation of Single Stage Axial Fans. NACA TM 1062, 1944.

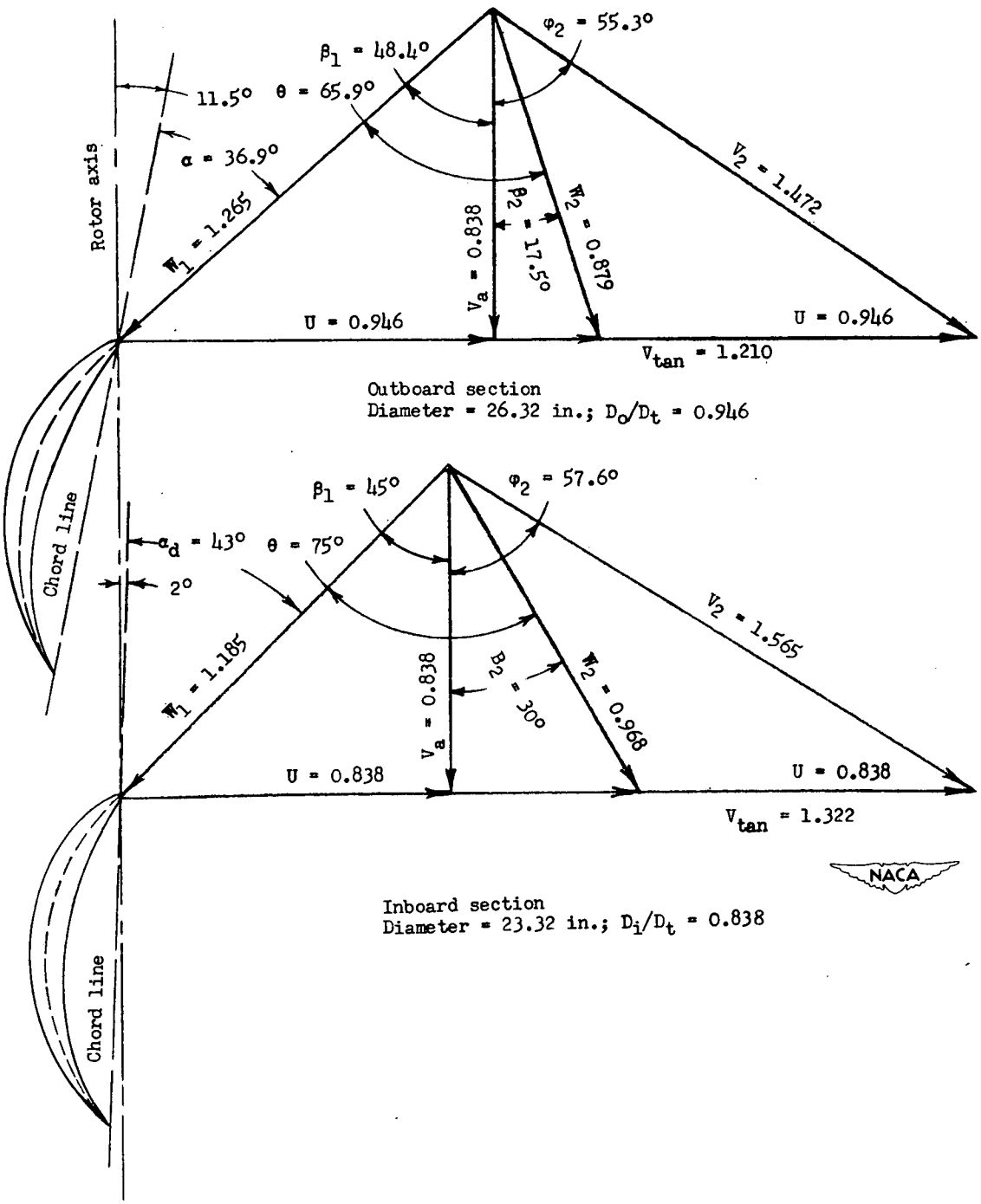

Figure 1.- Blade-angle and design-velocity diagrams for the inboard and outboard sections at the design blade-angle setting ζ_d. $U_t = 1.000$.

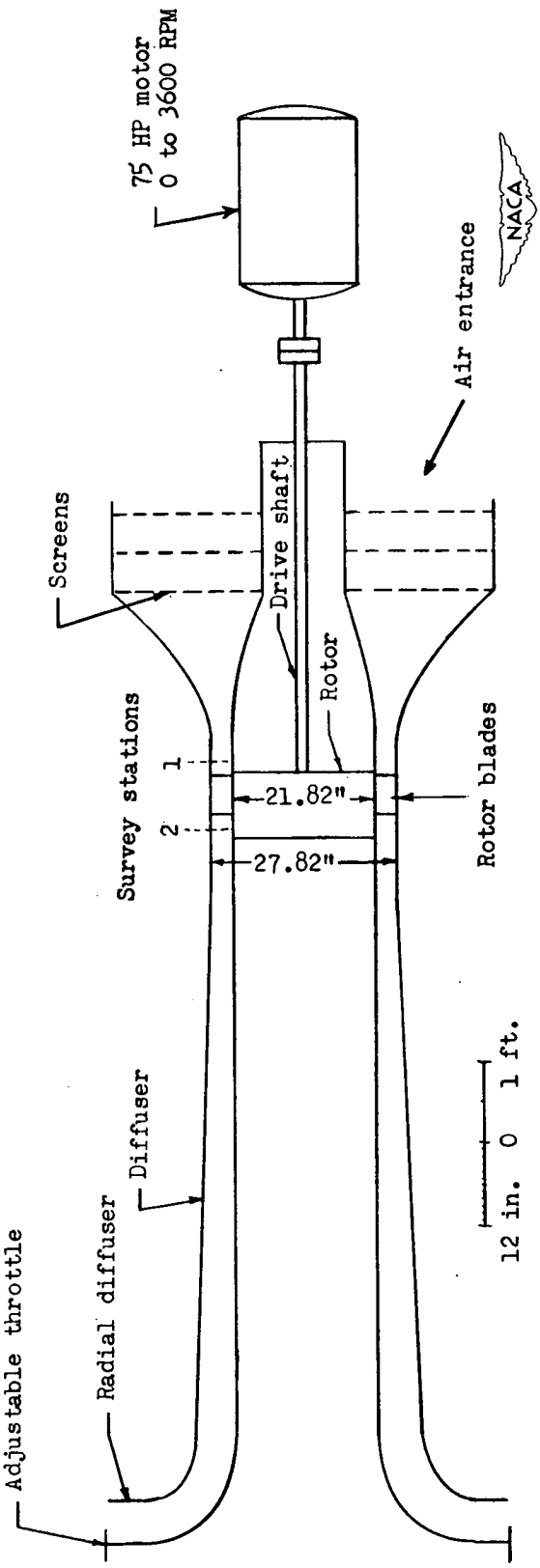

Figure 2.- Schematic diagram of test setup.

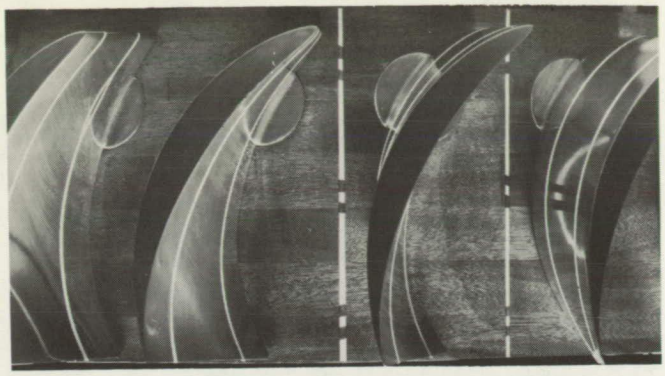

Blade setting 9° below design angle, ζ_d - 9°

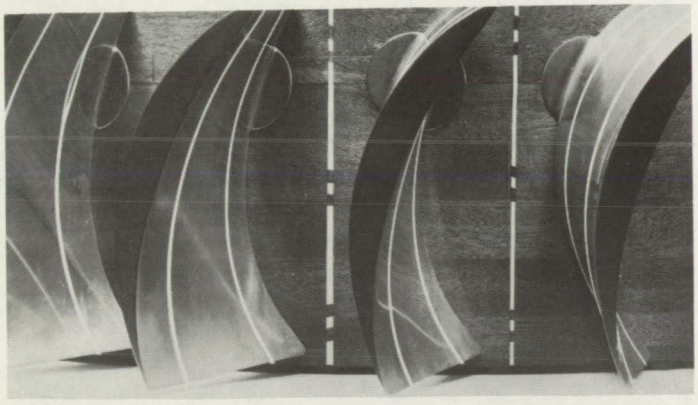

Design angle blade setting, ζ_d

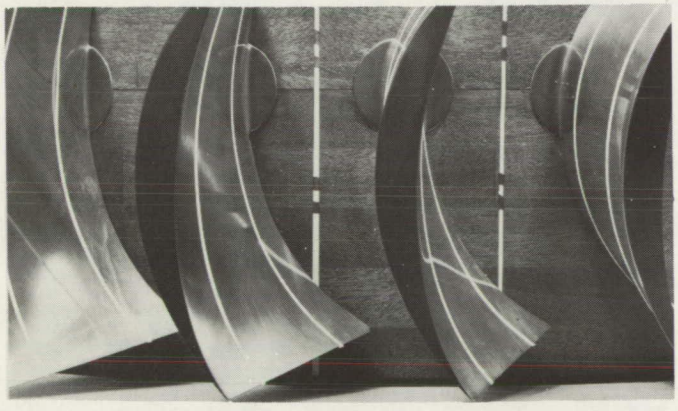

Blade setting 18° above design angle, ζ_d + 18°

Figure 3.- Model segment of the impulse blades and rotor showing the three settings used in performance tests with varying Φ. The lines on the blade indicate the positions of the inboard and outboard design blade sections, 25 percent height from hub and tip, respectively.

NACA
L-64904

Page intentionally left blank

Page intentionally left blank

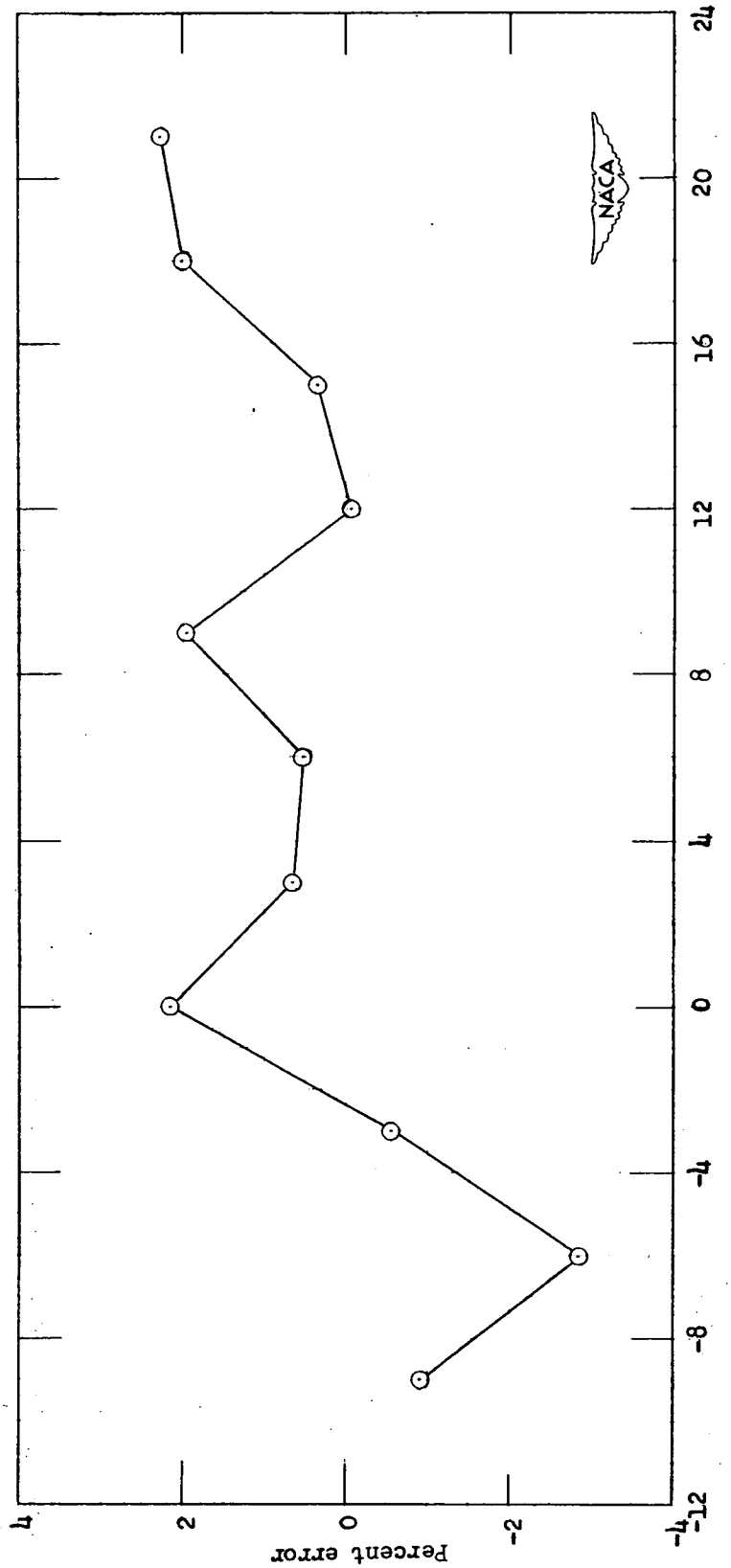

Figure 4.- Differences in measured weight flow of survey stations expressed as a percentage of station 2 weight flow at various blade-angle settings for the flow-inducing tests. $\Phi \cong 0.80$.

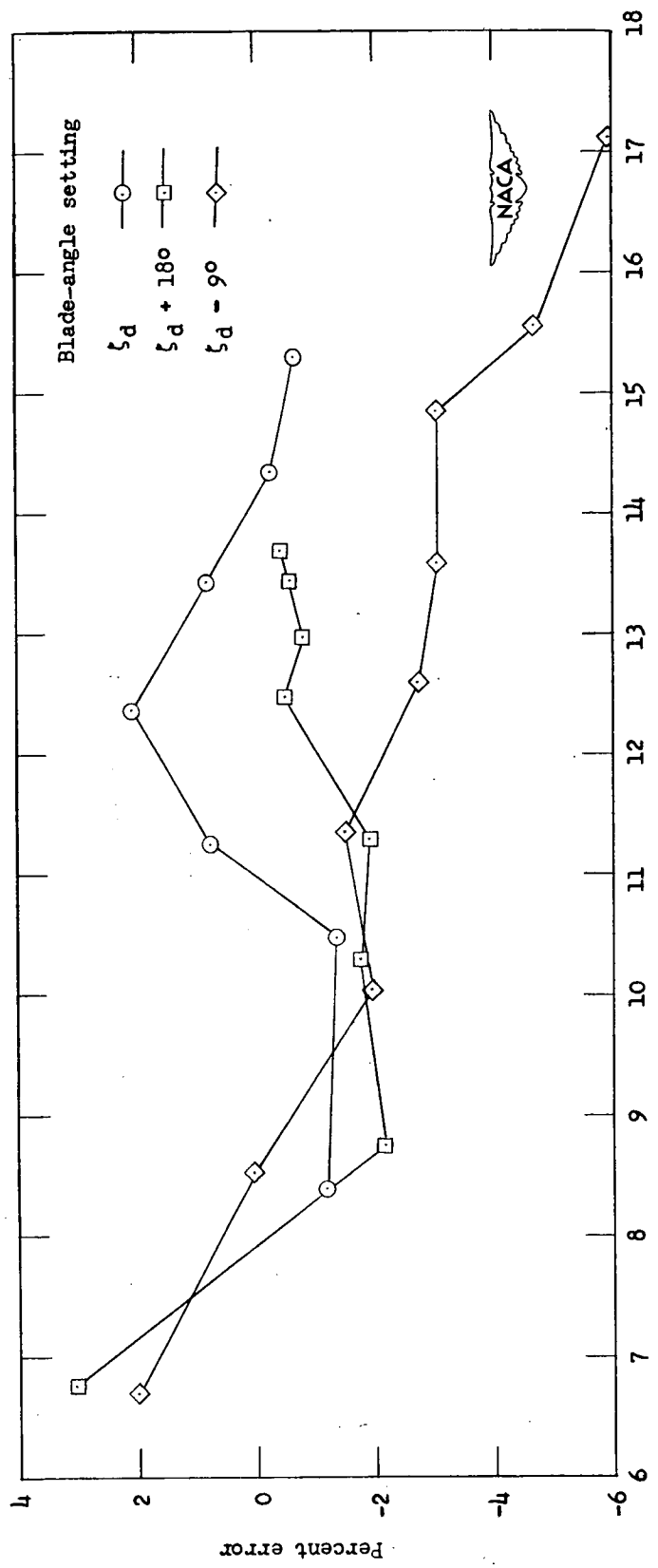

Figure 5.- Differences in measured weight flow of survey stations expressed in percentage of station 2 weight flow for the performance tests at three values of ζ.

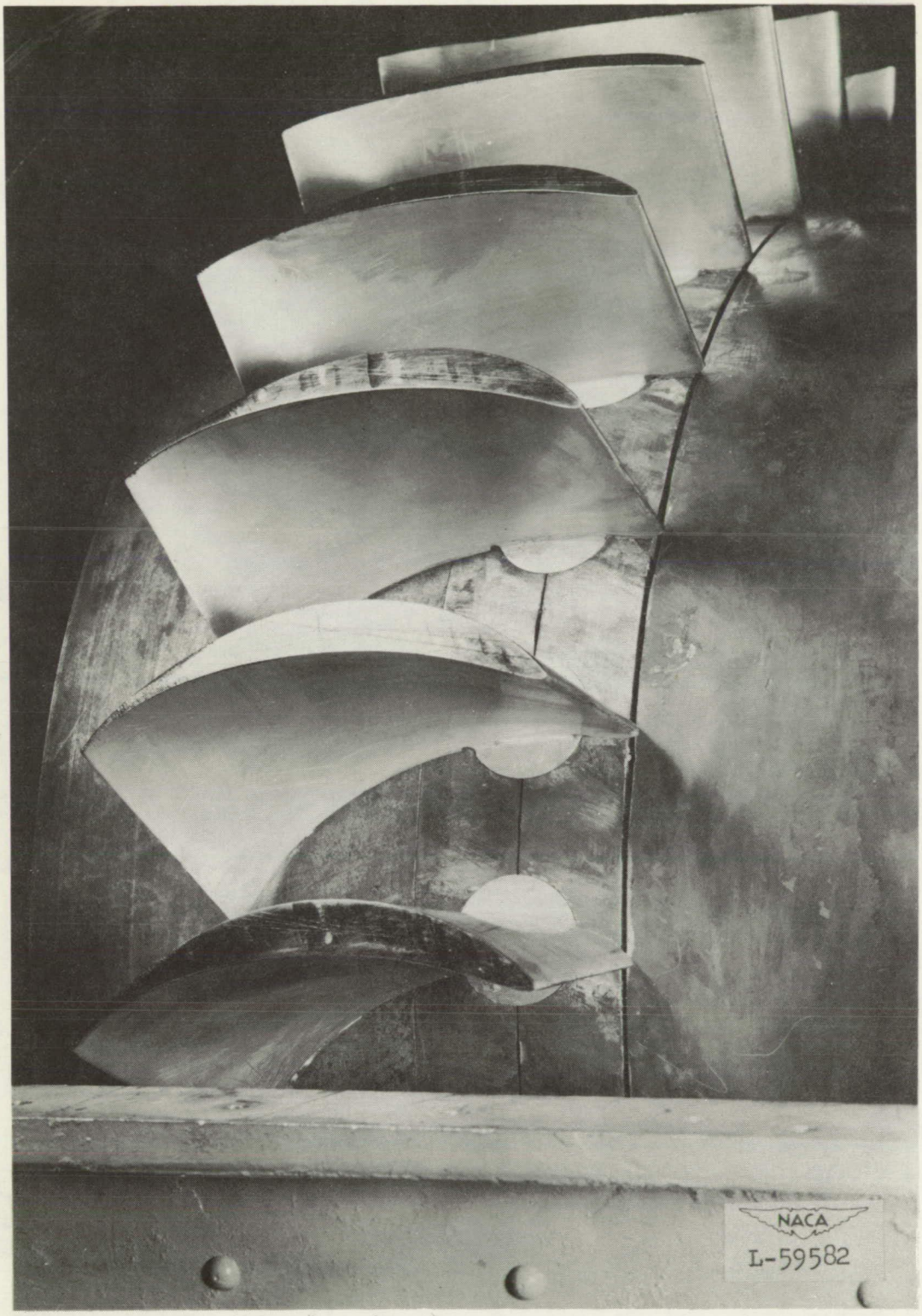

Figure 6.- Rotor assembly with the blade-angle setting 21° above ζ_d.

Page intentionally left blank

Page intentionally left blank

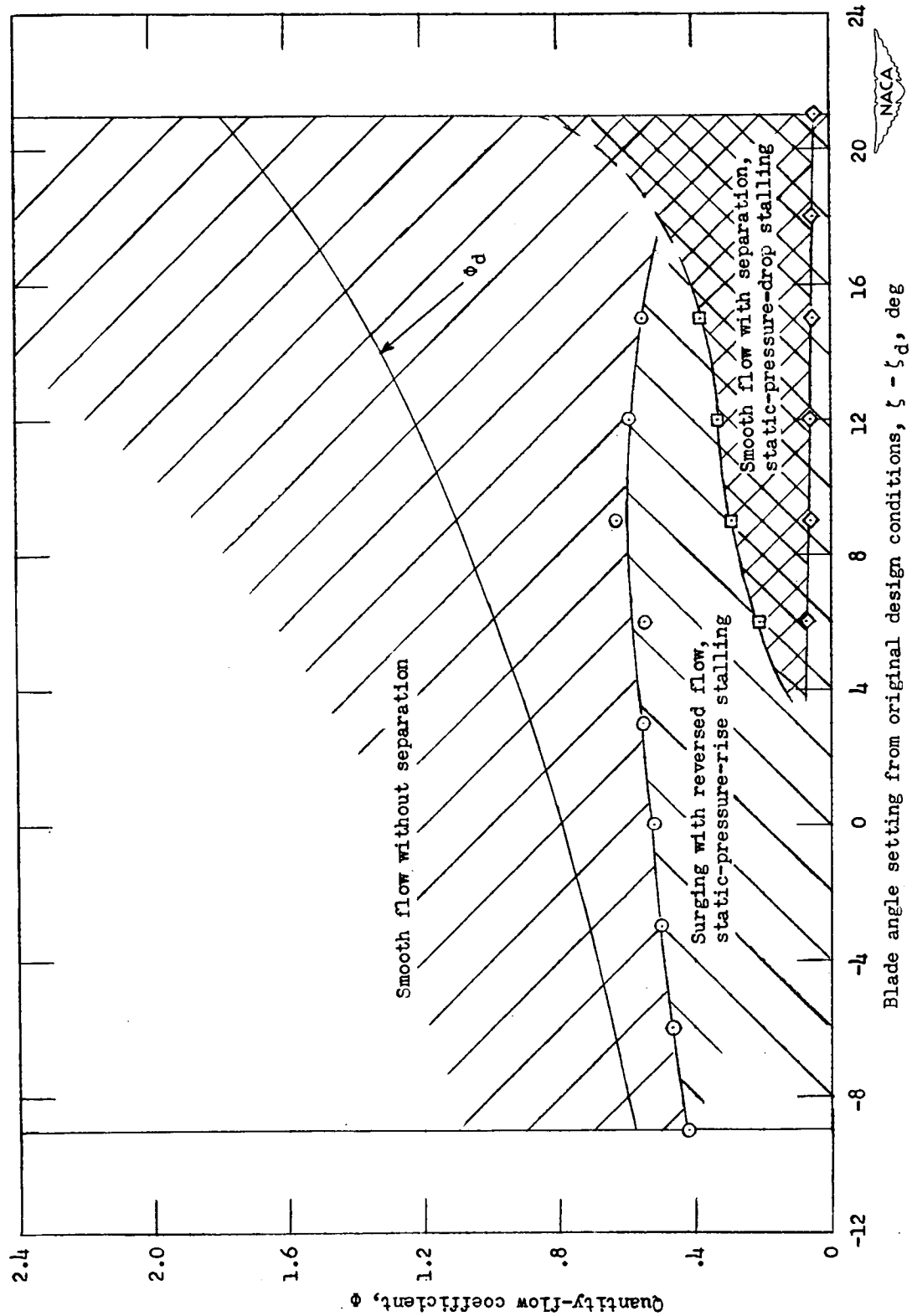

Figure 7.- Operating range for each flow pattern.

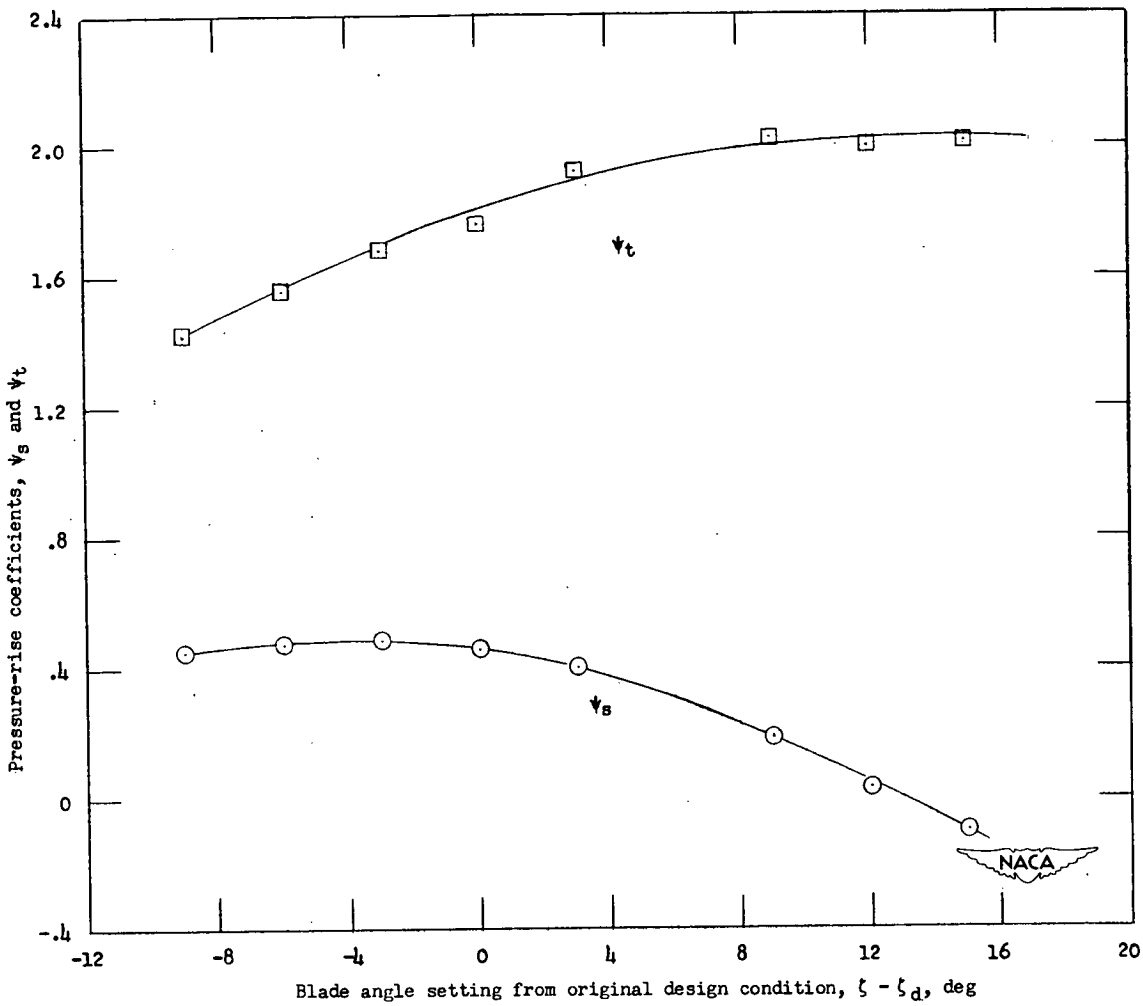

Figure 8.- Variation of total- and static-pressure-rise coefficients at mean diameter with blade-angle setting, just before stall conditions.

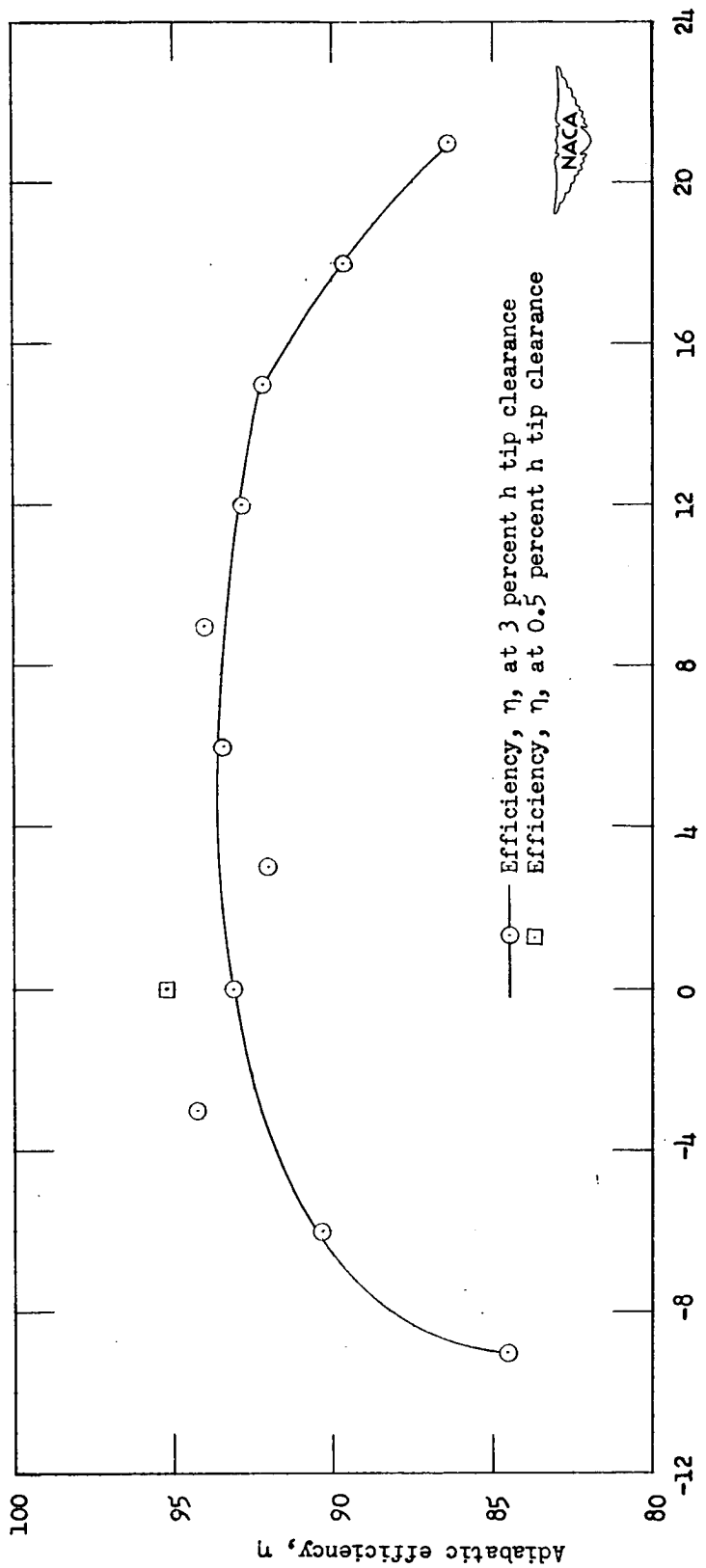

Figure 9.- Variation of efficiency with blade-angle setting for the flow-inducing tests. $\Phi \cong 0.80$.

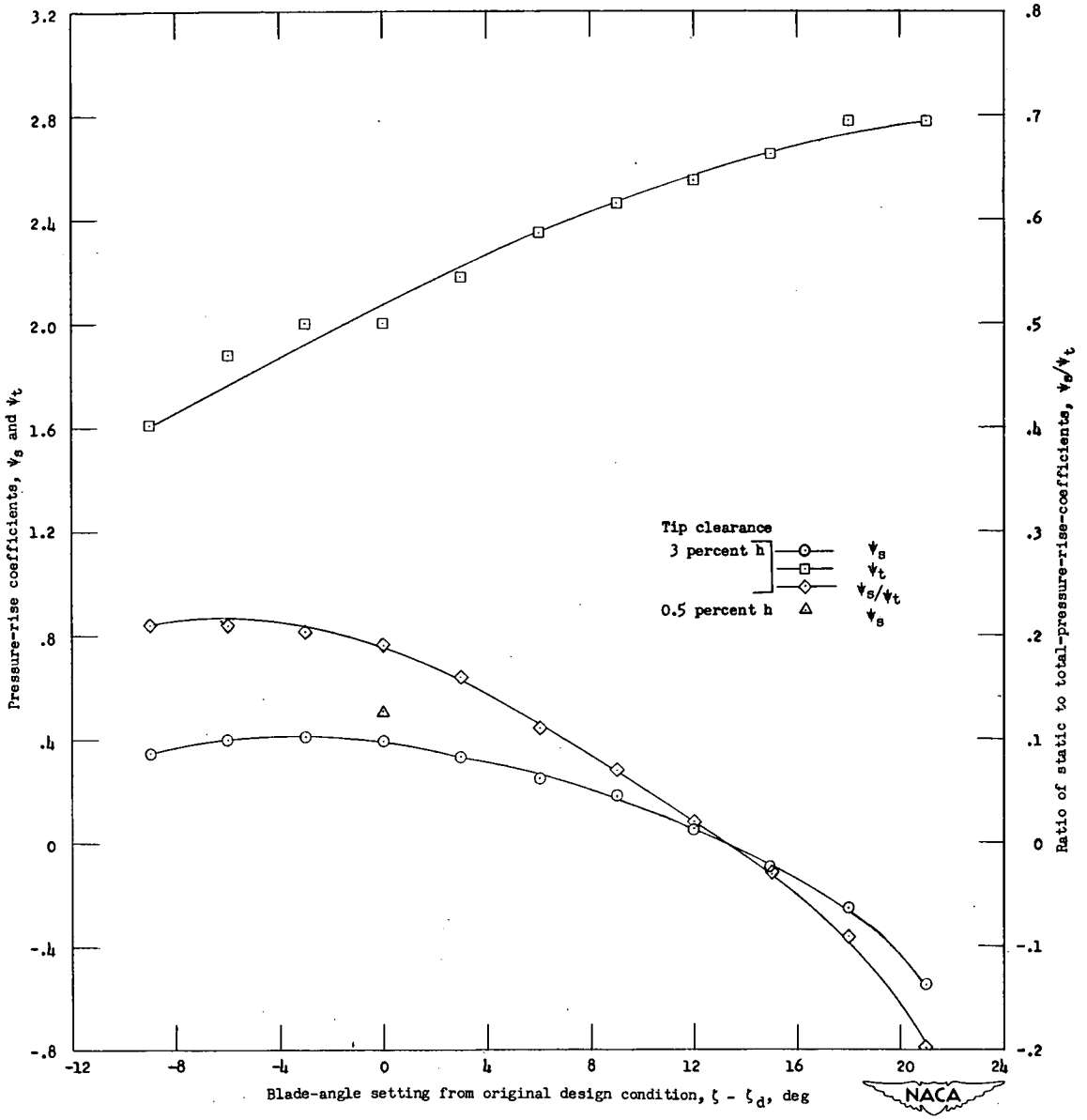

Figure 10.- Variation of total- and static-pressure-rise coefficients and the ratio of static- to total-pressure rise with blade-angle setting from the flow-inducing tests. $\Phi \cong 0.80$.

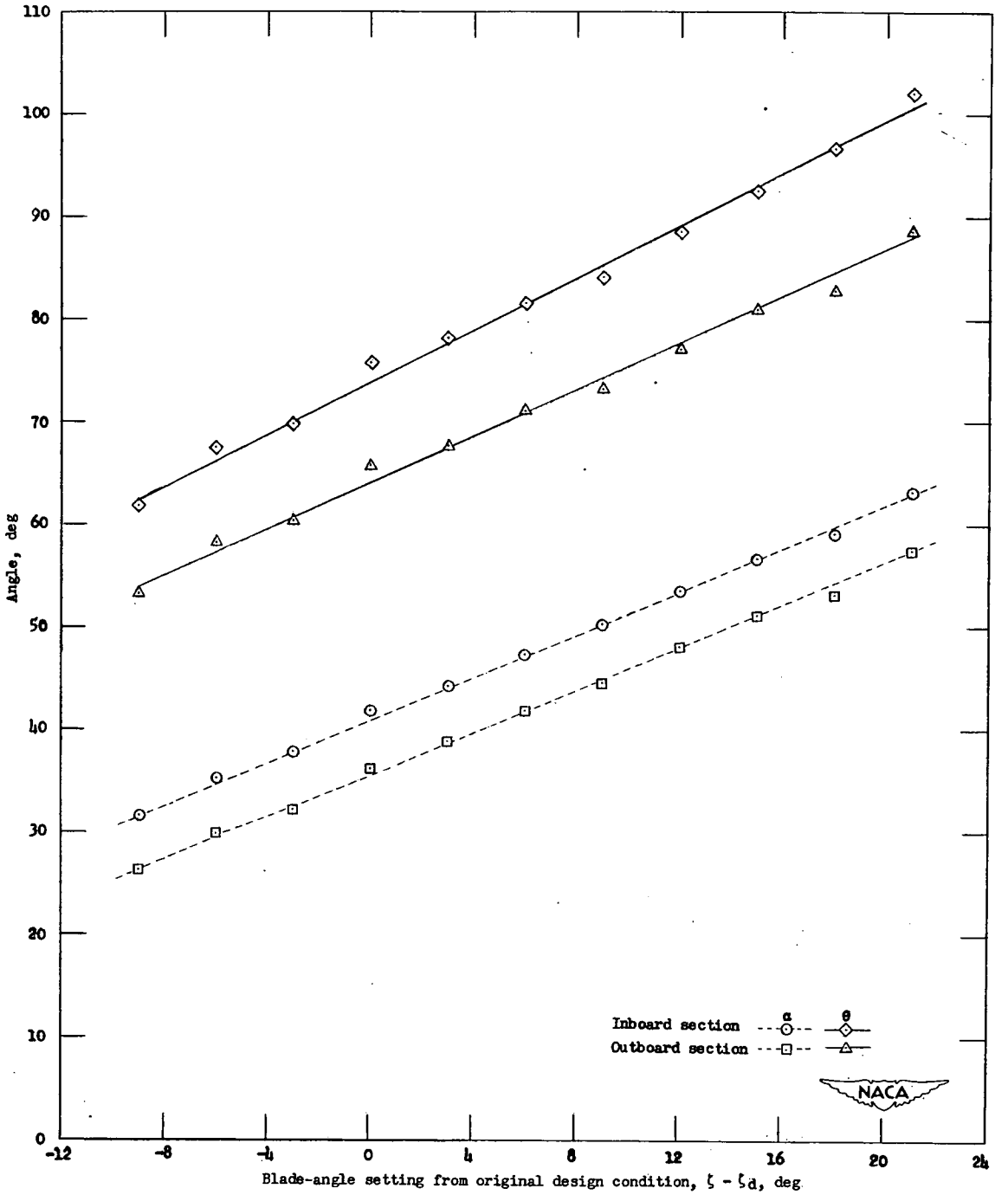

Figure 11.- Variation of turning angle θ and angle of attack α with blade-angle setting from the flow-inducing tests. $\Phi \cong 0.80$.

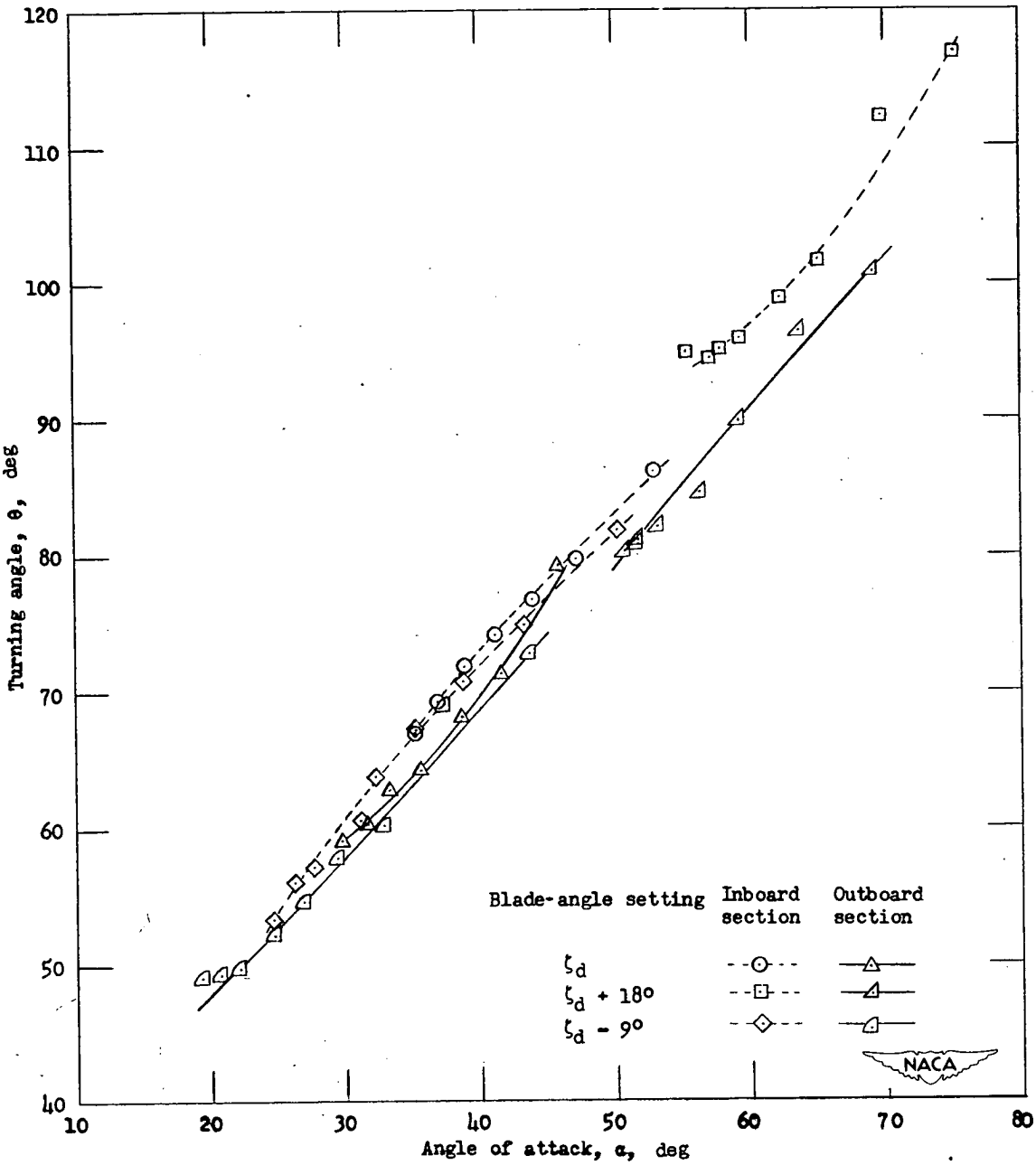

Figure 12.- Variation of turning angle with angle of attack at the two design sections from performance tests over a range of Φ for three values of ζ.

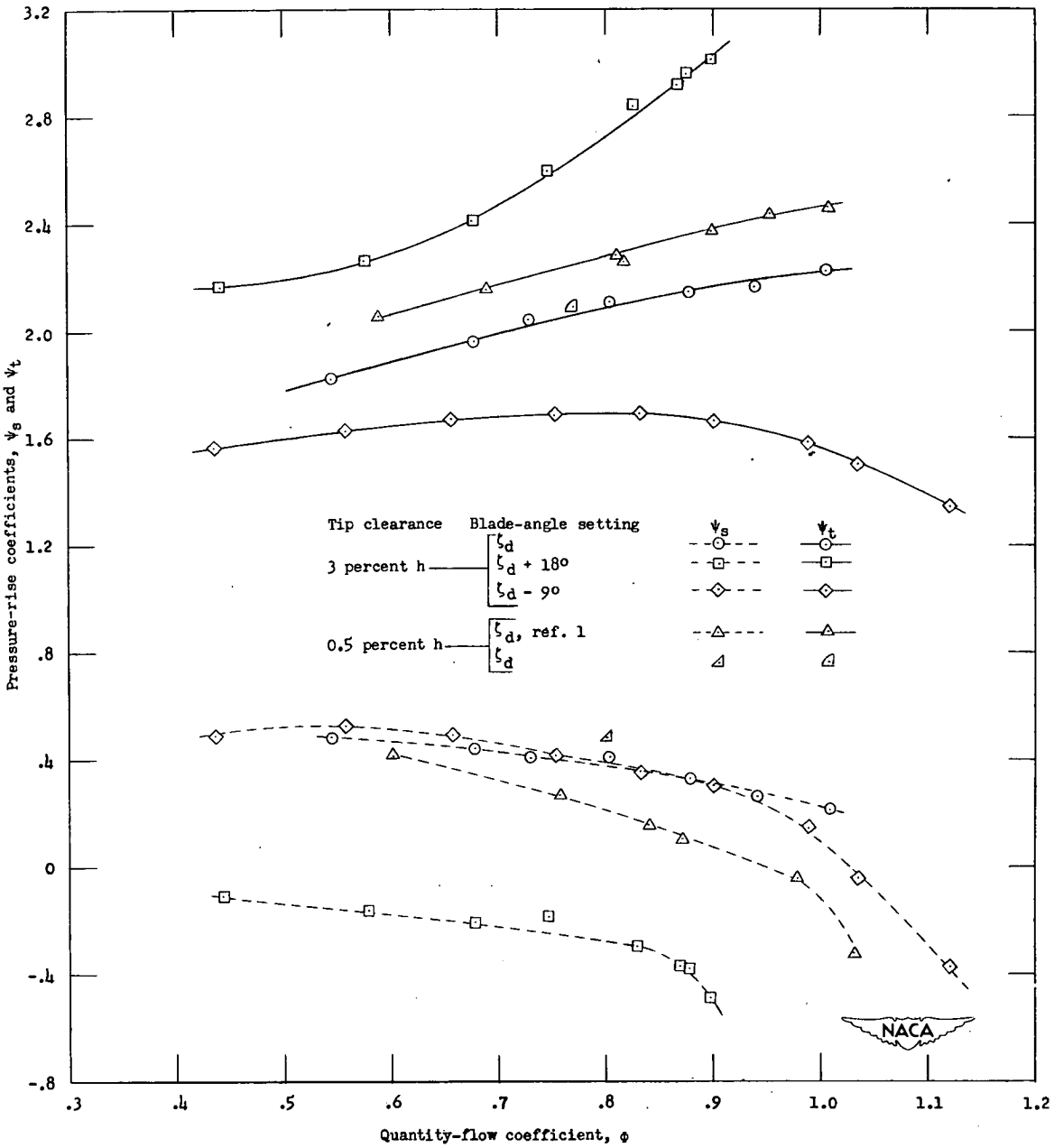

Figure 13.- Variation of total- and static-pressure-rise coefficients, ψ_t and ψ_s, with quantity-flow coefficient from the performance tests over a range of Φ at three values of ζ. Data from reference 1 included for comparison.

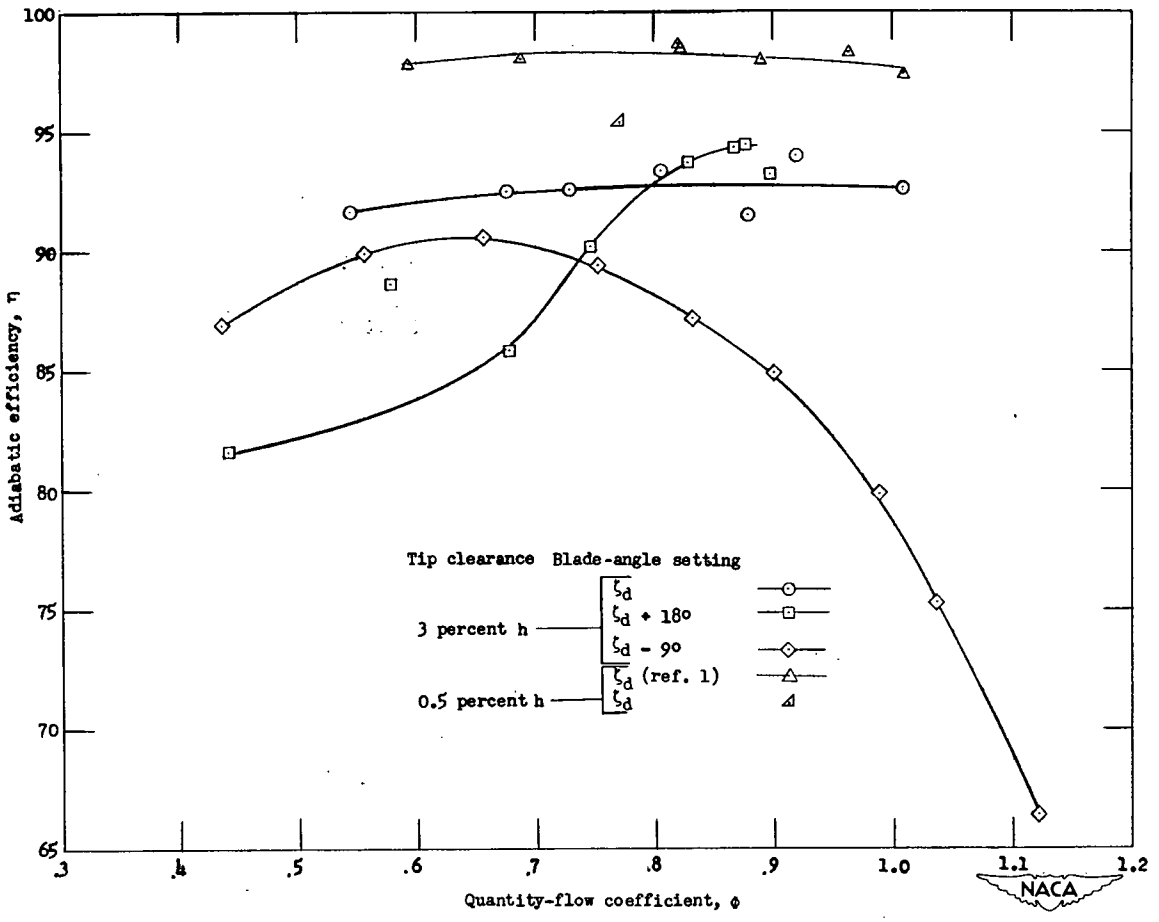

Figure 14.- Variation of efficiency with quantity-flow coefficient from the performance tests over a range of Φ at three values of ζ. Data from reference 1 included for comparison.

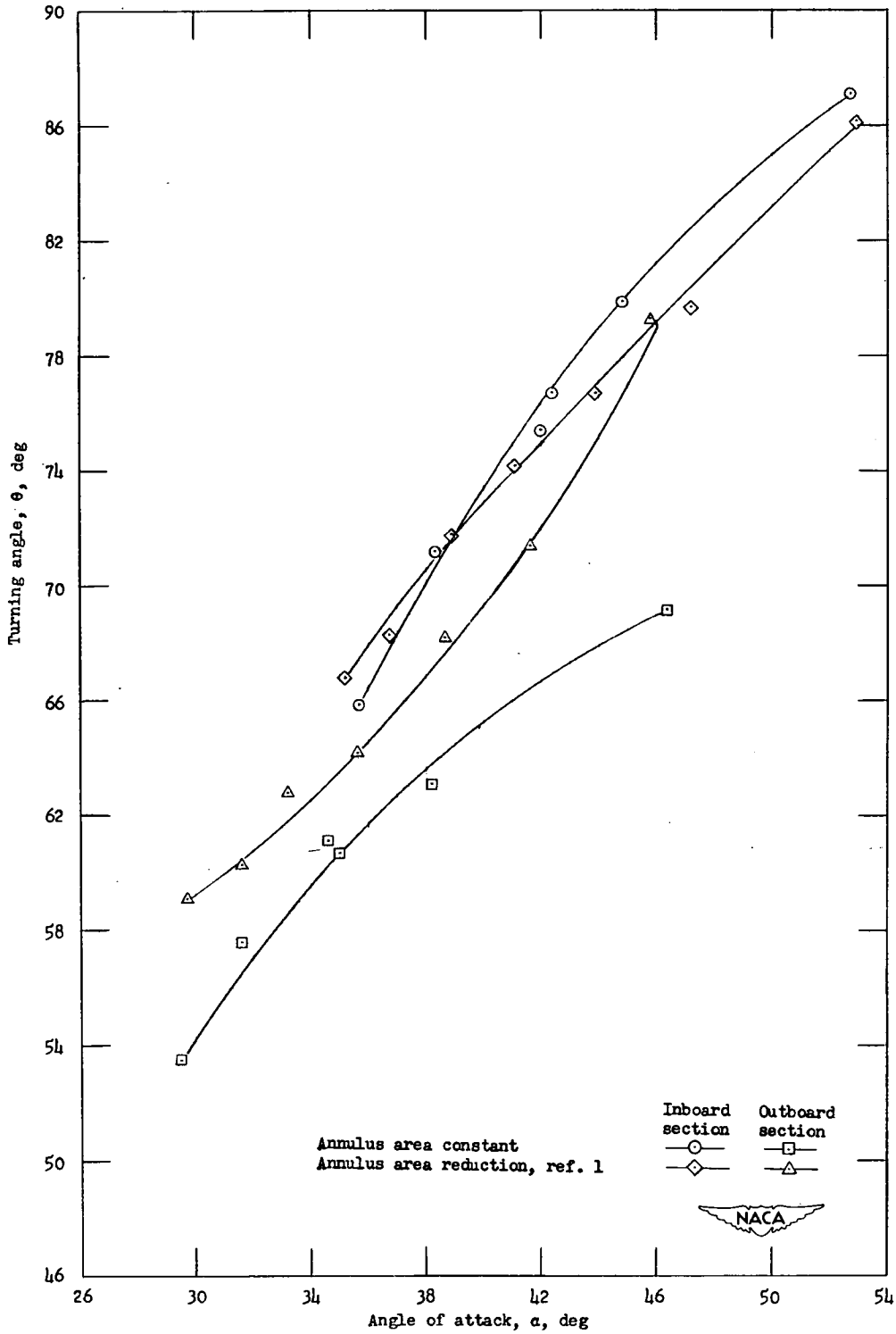

Figure 15.- Variation of turning angle θ with angle of attack α at the two design sections for the design blade-angle setting compared with the results from reference 1 with area reduction.

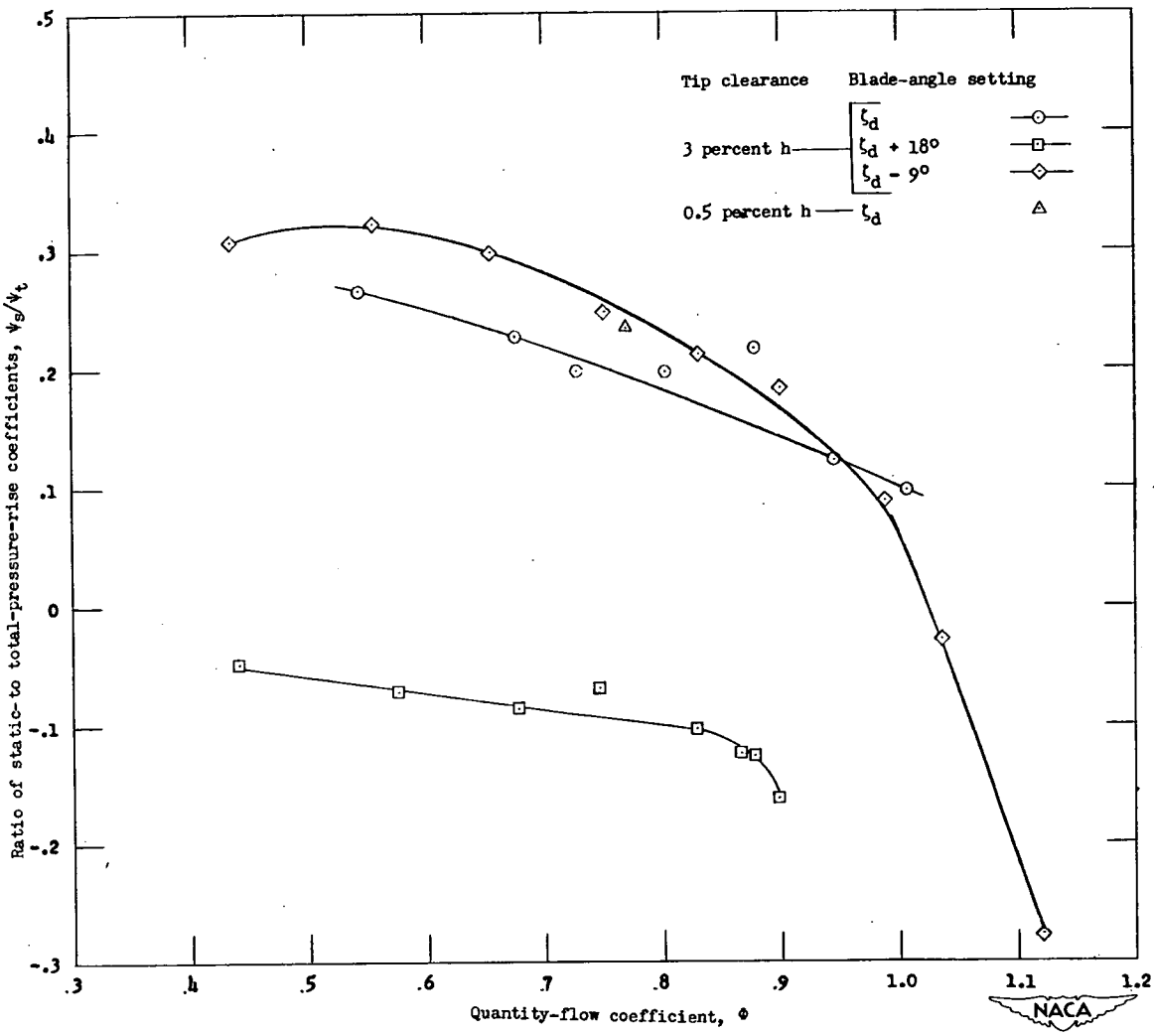

Figure 16.- Variation of the ratio of static- to total-pressure-rise coefficient with quantity-flow coefficient from the performance tests over a range of Φ at three values of ζ.